Macromolecular Research, Vol. 21, No. 1, pp 108-113 (2013)
DOI 10.1007/s13233-013-1055-0

www.springer.com/13233
pISSN 1598-5032 eISSN 2092-7673

In vitro Evaluation of UHMWPE/Zirconia Composite using Human Peripheral Blood Mononuclear Cells

Ki-Dong Yoo[1,4], Gee-Hee Kim[1,4], Dong Il Noh[2], Ju Woong Jang[2], Young Bok Shim[2], and Heung Jae Chun*[,3,4]

[1]*Department of Internal Medicine, College of Medicine, The Catholic University of Korea, Gyeonggi 442-723, Korea*
[2]*Research Institute of Biomedical Engineering, Korea Bone Bank Co. Ltd., Seoul 153-782, Korea*
[3]*Department of Biomedical Sciences, College of Medicine, The Catholic University of Korea, Seoul 137-701, Korea*
[4]*Institute of Cell & Tissue Engineering, College of Medicine, The Catholic University of Korea, Seoul 137-701, Korea*

Received June 4, 2012; Revised June 25, 2012; Accepted June 29, 2012

Abstract: The objective of the present study was to investigate *in vitro* biocompatibility of ultra high molecular weight polyethylene (UHMWPE)/zirconia-polymerized composite (PC) using human peripheral blood mononuclear cells (PBMCs). This study was undertaken to compare the levels of free radical generations for neat UHMWPE and PC through irradiation sterilization, and their response to PBMCs viability. Electron spin resonance (ESR) studies showed that γ-ray irradiation of the samples generated free radicals; the extent was inversely related to zirconia content, and the free radicals strongly influenced cell viability. DNA fragmentation and DAPI staining assays revealed that cell death was associated with the induction of apoptosis. Flow cytometry also showed that cell death was largely dependent upon both early and late apoptosis, and, importantly, oxidized PC (ox-PC) exhibited a significantly lower rate for late apoptosis compared to that of oxidized UHMWPE (ox-UHMWPE).

Keywords: ultra high molecular weight polyethylene, zirconia, composite, peripheral blood mononuclear cells, free radicals, cytotoxicity, apoptosis.

Introduction

Ultra high molecular weight polyethylene (UHMWPE) has been widely used as a suitable bearing material for manufacturing knee and hip joints, because it satisfies the artificial joint material requirements of a low friction coefficient and a high wear rate, as well as an excellent chemical resistance, high mechanical strength, and bio-inertness.[1-6] For sterilization of UHMWPE before implantation, the ionizing radiations such as gamma and electron beam are extensively used, because the radiations not only provide a convenience, but also benefit the polyethylene cross-linking, which improves the wear properties.[5,6] However, the generation of free radicals formed by irradiation leads the oxidation of UHMWPE and, within 6~8 years of implantation, produces the reactive oxygen species (ROS), which is responsible for change of mechanical property and a strong inflammatory response, consequently prosthesis failure.[5,6] Although direct contact of human osteoblast-like cells and fibroblast with oxidized UHMWPE (ox-UHMWPE) is able to alter the release of matrix metalloproteinase for the extracellular matrix remodeling.[7,8] It is generally recognized that ROS recruits peripheral blood cells, macrophages, and multi-nucleated cells, resulting in acute and chronic inflammatory reactions.[9] In addition, the increased cellular ROS levels have been shown to be associated with induction of apoptotic and necrotic cell death.[10] Apoptosis, as a non-inflammatory pathway, is a physiological mode of cell death under genetic control without causing damage to the surrounding tissues, whereas necrosis is characterized by loss of membrane integrity and release of potentially toxic intracellular contents.[11] The toxic intracellular contents released from necrotic cells produce "secondary necrosis" mainly responsible for osteolysis and loosening of prosthesis.[12]

A previous study reported that UHMWPE/zirconia polymerized composite (PC) prepared by the *in situ* polymerization of ethylene using a Ti-based Ziegler-Natta catalyst markedly decreased the oxidation index compared to neat UHMWPE by changing chemical composition and crystallinity.[13] Because the level of ROS due to UHMWPE oxidation entirely depends on the content of free radicals, investigation of the cytotoxicity level and the cell death pathway triggered by the oxidized samples is critical.

The aim of this study was to compare the free radical generations of UHMWPE and PC by the irradiation sterilization, and their effects on the viability of human peripheral blood mononuclear cells (PBMCs) as an *in vitro* biocompatibility test for long-term implants.

*Corresponding Author. E-mail: chunhj@catholic.ac.kr

Experimental

Preparation of UHMWPE and UHMWPE/Zirconia Polymerized Composites (PCs). A series of PCs (15, 23, and 43 wt% of zirconia; designated as PC15, PC23, and PC43, respectively) were synthesized in the presence of $TiCl_4$ and Et_3Al in a high pressure glass reactor as described previously.[13] The commercial UHMWPE (Mipelon™ XM-220, Mitsui Chem., Tokyo, Japan) was used as a standard for comparison with the PCs.

Determination of Free Radical Generation. The electron spin resonance (ESR) spectroscopy was employed to determine the content of free radicals in the samples. The specimens were microtomed into 200-μm thick slices, cut into strips of 3×20 mm^2, and exposed to ^{60}Co γ-rays, accumulating a dosage of 25 kGy at 10 kGy/h (IR221n wet storage type C-188, MDS Nordion, CA, USA) at room temperature. ESR spectra of irradiated samples were obtained from samples in 5-mm NMR tubes, on a JEOL TE-300 ESR spectrometer (JEOL, Tokyo, Japan), which operated 9.435 GHz microwave at 1 mW power and 100 kHz magnetic field modulation frequency. The spectral double integration method was used to determine the relative free radical concentration (FRC) of the samples.

Isolation and Culture of PBMCs. Human whole blood samples from young healthy donors were centrifuged at 2,500 rpm for 15 min. Buffy coat was collected and added to 1 mM EDTA (Sigma, MO, USA) containing RPMI 1640 (Gibco, NY, USA) supplemented with 10% fetal bovine serum (FBS, Gibco, PA, USA), 1% penicillin-streptomycin (PS, Gibco, NY, USA) and 2 mM *L*-glutamine (Sigma, MO, USA). The collected buffy coat was then loaded into Lymphoprep™ solution (Axis- Shield, Oslo, Norway) and centrifuged at 2,300 rpm for 15 min. The middle layer was collected, mixed with 1 mM EDTA-RPMI 1640 medium, and re-centrifuged at 1,500 rpm for 15 min. The supernatant was removed, and the remaining pellet was washed by centrifugation with sterile phosphate buffer solution (PBS, pH 7.4) several times. The resultant pellet containing mononuclear cells was cultured in RPMI 1640 medium.

Cell Viability. The viability of cells in the samples was determined by WST-1 (Roche Diagnostics Ltd, Lewes, UK) test. The specimens, microtomed into 200-μm thickness before and after irradiation, were circularly punched into 4 mm in diameter, placed in 96-well plates, and sterilized. Subsequently, primary cultured PBMCs (1×10^5 cells) were seeded into each well. After incubation for 48 h, viability of PBMCs was measured using WST-1 by micro plate reader (Spectra Max 250, Molecular Devices, CA, USA).

DAPI Staining. In order to assess nuclear morphology, cells were stained with 4′,6′-diamidino-2-phenyllindole (DAPI, Probes, OR, USA). Prior to staining, microtomed samples were circularly punched into 3 cm in diameter and placed in a 6-well plate. PBMCs (1×10^5 cells) were seeded into each well, incubated for 24 h, and washed with PBS. DAPI staining was performed in DNA staining buffer (10 mM pipes, pH 6.8, 2 mM $MgCl_2$, 100 mM NaCl, 0.1% (v/v) Triton X-100) containing 2 μg/mL 4′,6′-diamidine-2′-phenylindole dihydrochloride (DAPI) for 30 min at room temperature. Images of the stained nuclei were visualized for apoptotic changes in the chromatin by a fluorescence microscope (TR-62A02, Olympus, Tokyo, Japan) at 460-500 nm.

DNA Fragmentation. DNA fragmentation was assayed to evaluate apoptosis by agarose gel electrophoresis. After 24 h of incubation with the samples, as described in previous section, PBMCs were harvested, washed with PBS (pH 7.4), and lysed in 0.5 mL of lysis solution (0.5% SDS, 25 mM EDTA, and 100 mM NaCl) containing 100 μg/mL of proteinase K (Promega, Southampton, UK) for 3 h at 55 ºC. The denatured proteins were extracted with phenol-chloroform (1:2), and the nucleic acids were precipitated with ethanol. The pellet was dissolved in 50 μL TE buffer at 37 ºC for 1 h. The DNA samples were electrophoresed on a 1.5% agarose gel at 5 V/cm and stained with ethidium bromide (EtBr, Sigma, Steinheim, Germany) to visualize DNA fragments.

Flow Cytometry. PBMCs (1×10^5 cells) in each sample were incubated at 37 ºC in 5% CO_2 environment for 48 h. One milliliter of serum-free RPMI 1640 was added to each sample, followed by 24 h of incubation, and centrifugation at 1,200 rpm for 15 min. The resultant pellet was washed with PBS, and 5 μL of 1×binding solution containing Annexin V (BD Pharmingen, CA, USA) was added. The sample was incubated for 15 min in a dark room, and subsequently 5 μL propidium iodide (PI, BD Pharmingen, CA, USA) solution was added. After 15 min of incubation at room temperature, each sample was analyzed by the flow cytometry (FACS Vantage SE, BD Biosciences, CA, USA) equipped with a 15-mW air-cooled argon ion laser operating at 488 nm. PI red fluorescence was detected through a 620-nm BP filter and displayed on a four-decade log scale. Apoptotic and necrotic cells were quantified by counting the number of cells in dot plot showing PI, Annexin, and PI/Annexin double positive fluorescences.

Statistical Analysis. All quantitative data were expressed as the mean±standard deviation. Statistical analysis was performed with one-way analysis of variance (ANOVA) using SPSS software (SPSS Inc., IL, USA). A value of $p < 0.05$ was considered statistically significant.

Institutional Review Board (IRB). This study has been reviewed and approved by the IRB (MC12DNMI0028) at Catholic University.

Results and Discussion

ESR. The ESR spectra of γ-ray irradiated samples with respect to the zirconia contents are shown in Figure 1. Besides the peak intensity, the spectra showed similar reso-

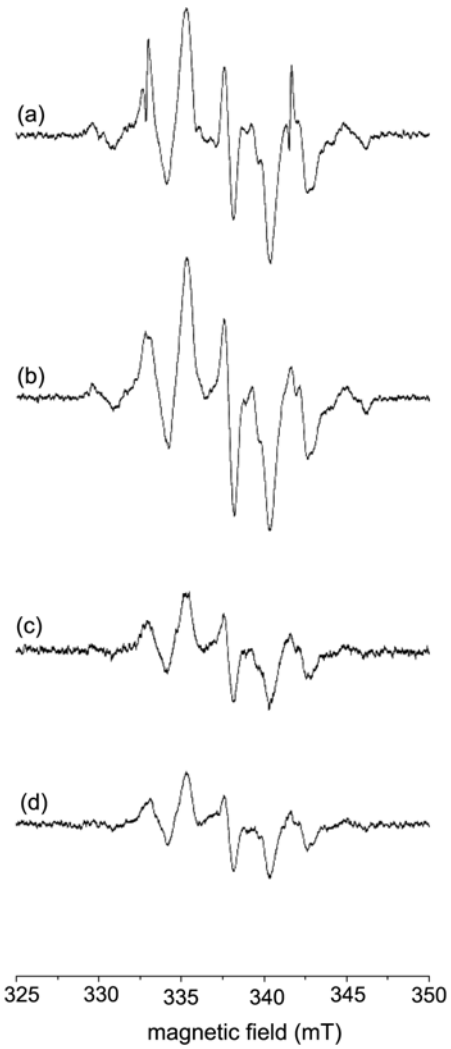

Figure 1. ESR spectra of γ-ray irradiated neat UHMWPE and polymerized composites (PCs): (a) UHMWPE, (b) PC15, (c) PC23, and (d) PC43.

nance signals. The spectra consist of seven resonance lines with hyperfine coupling constant ΔH=5G, line width ΔW= 2G, and *g*-value of 2.004. The basis of ESR spectroscopy is the absorption of electromagnetic radiation by unpaired electrons in a magnetic field.[14] Unpaired electrons are characterized by an angular momentum, the 'spin', which is connected with a magnetic moment. Ordinary molecules have a total electron spin of zero (singlets). On the other hand, radicals have a total electron spin of 1/2 corresponding to one unpaired electron (doublets), and triplet states with two unpaired electrons have an electron spin of 1. In order to observe resonance absorption of electromagnetic radiation, a magnetic field, which acts on the elementary magnetic moments of the electrons or nuclei, is necessary. The force of this interaction is proportional to the magnetic flux density **B** of the field and to the magnetic dipole moment μ of the electron. The resonance condition in its general form is given as: $h\upsilon=g\mu\mathbf{B}$, where *h*=Planck's constant and *g*=proportionality factor (*g* factor). A free electron spin is expected to have a *g* value of 2.0. In real materials, *g* may differ from this value, depending on the variations in the coupling between the spin and orbital angular momentum. In the case of polyethylene, primary products of irradiation are alkyl radicals (*g* value of 2.0027), which undergo crosslinking and chain scission or transform to more stable allyl radicals (*g* value of 2.0026).[15] In air, the peroxy radicals (*g* value of 2.0156) are the primary product of oxidation. These radicals finally produce the oxidation products such as alcohols, aldehydes, ketones, carboxylic acids, and esters. The overall reaction is known as the Bolland's cycle, and *g* value of oxidized polyethylene reaches to 2.004.[16]

Table I. Relative Free Radical Concentration (FRC)

	Area	Relative FRC
UHMWPE	5905.352	1.000
PC15	3900.569	0.661
PC23	1745.315	0.296
PC43	1233.612	0.209

Table I shows the ESR peak area of the samples calculated by double integration, and the relative FRC of the samples, under the assumption that the peak area of the neat UHMWPE is in unity. The relative FRC of the samples decreased with increase in the content of zirconia. Previously, the effects of zirconia content on the oxidation behavior of the γ-ray treated UHMWPE/zirconia composite were extensively investigated.[13] The oxidation indices of the samples decreased with the increase in the zirconia contents. The differential scanning calorimetry (DSC) results indicated that the crystallinity of the samples gradually increased with the increase in the contents of zirconia. In addition, the transmission electron microscopies of the samples showed that the zirconia particles were uniformly dispersed throughout the whole matrix up to 43 wt% of zirconia content. Consequently, the decreased oxidative behavior was attributed to the increased crystallinity as well as the decreased polymer portion of the UHMWPE/zirconia composites. In the same manner as the oxidative index, the extents of free radicals of the samples have to be inversely related to the concentration of zirconia, because free radical is the source of the oxidation.

Viability of PBMCs. Cytotoxicity of PBMCs due to the contact with the samples was evaluated by WST-1 test. Figure 2 shows the WST-1 reduction in PBMCs in the presence of the samples. The WST-1 reduction capacities of the samples without irradiation, UHMWPE and PCs, were found to be very close to that of (-) control, polystylene plate without sample, irrespective of the zirconia content. For the oxidized samples, ox-UHMWPE and ox-PCs, oxidation of UHMWPE significantly reduced viability of PBMCs, and the MTT

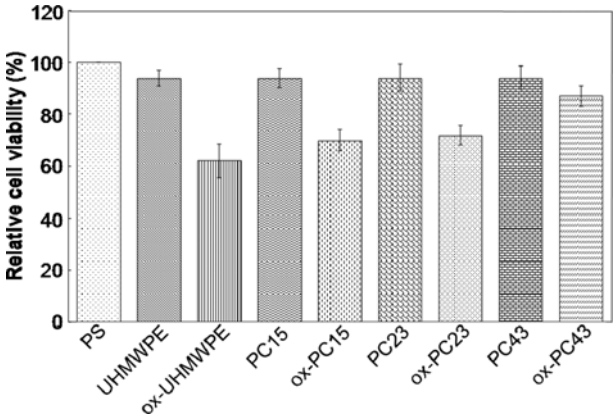

Figure 2. Relative viability of PBMCs due to the incubation with the samples.

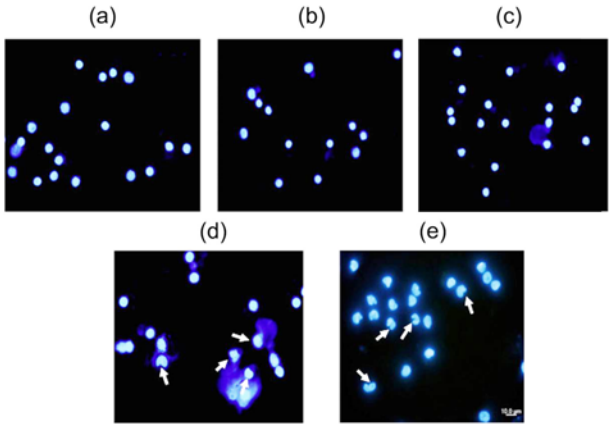

Figure 4. Detection of apoptosis by a DAPI staining: (a) PS, (b) UHMWPE, (c) PC43, (d) ox-UHMWPE, and (e) ox-PC43. The fragmented nuclei are indicated by arrows.

reduction capacity was inversely associated with the level of the free radical generation in the order of ox-PC43, ox-PC23, ox-PC15, and ox-UHMWPE. Therefore, we hypothesized that PC43 subjected to oxidation for sterilization would be able to alleviate cell death at the maximum due to the lowest level of the free radical generation on the surface.

Nuclear Analysis. A cell exposed to severe oxidative stress by the reactive oxygen species (ROS) may die. Although cell death occurs by multiple mechanisms, the mechanisms can be narrowed down into two basic mechanisms; necrosis and apoptosis.[17] During necrotic cell death, the cell swells and ruptures, releasing its contents into the surrounding area, thereby affecting adjacent cells. In the case of inflammatory cells, necrosis releases intracellular contents, which damages the surrounding cellular and/or tissue components leading to chronic inflammation conditions. Whereas, in apoptosis, the cells are activated by their own intrinsic suicide mechanism; thus, apoptosing cells do not release their contents, and apoptosis does not, in general, affect the surrounding cells. Therefore, the investigation of the mechanisms involved in PBMCs' death due to ROS has an important significance in assessing the biocompatibility of the samples. Apoptosis is characterized by cell shrinkage and DNA fragmentation due to the activation of a caspase-dependent DNA endonuclease, which cleaves the genomic DNA into nucleosome-sized units.[18] In order to evaluate whether the growth inhibition due to the contact with the irradiated samples is linked to apoptosis, the induction of apoptosis was identified by DNA fragmentation patterns in multiples of 180-200 bp of oligonucleosomal DNA fragments, using agarose gel electrophoresis (Figure 3). The cells exposed to the samples before irradiation exhibited no DNA fragmentation; however, a clear multiple pattern of apoptotic DNA was observed from PBMCs exposed to the oxidized samples. To further substantiate apoptosis of PBMCs, DAPI staining was performed, because nucleosomal DNA fragmentation can be directly visualized by staining the nuclei of cells with DAPI for the morphological consequences of exposure to the oxidized samples: the apoptotic cells generally exhibit morphological changes by DAPI staining due to the induced DNA condensation as well as the induced DNA damage.[18] Figure 4 represents the fluorescence microscopy of PBMCs stained by DAPI. The cells incubated on (-) control exhibited homogeneously round shaped healthy nucleus. The cells exposed to the samples, UHMWPE and PC43 before irradiation, exhibited no morphological alterations compared to (-) control. In contrast to cells on neat samples, among the PBMCs treated with the ox-UHMWPE and ox-PC43, typical apoptotic morphological changes with irregular and fragmented shape of nuclei namely apoptotic bodies were observed by fluorescence microscopy after staining the nuclei of cells with DAPI. This demonstrates that the oxidation process of the samples would be able to increase apoptosis of cells. However, apoptotic induction by ox-PC43 was lower than that by ox-UHMWPE.

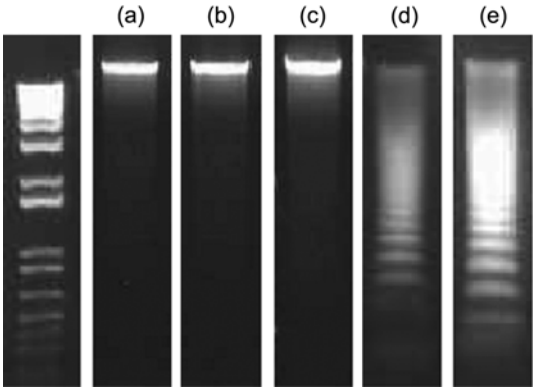

Figure 3. Detection of apoptosis by DNA fragmentation upon treatment with the samples: (a) PS, (b) UHMWPE, (c) PC43, (d) ox-UHMWPE, and (e) ox-PC43.

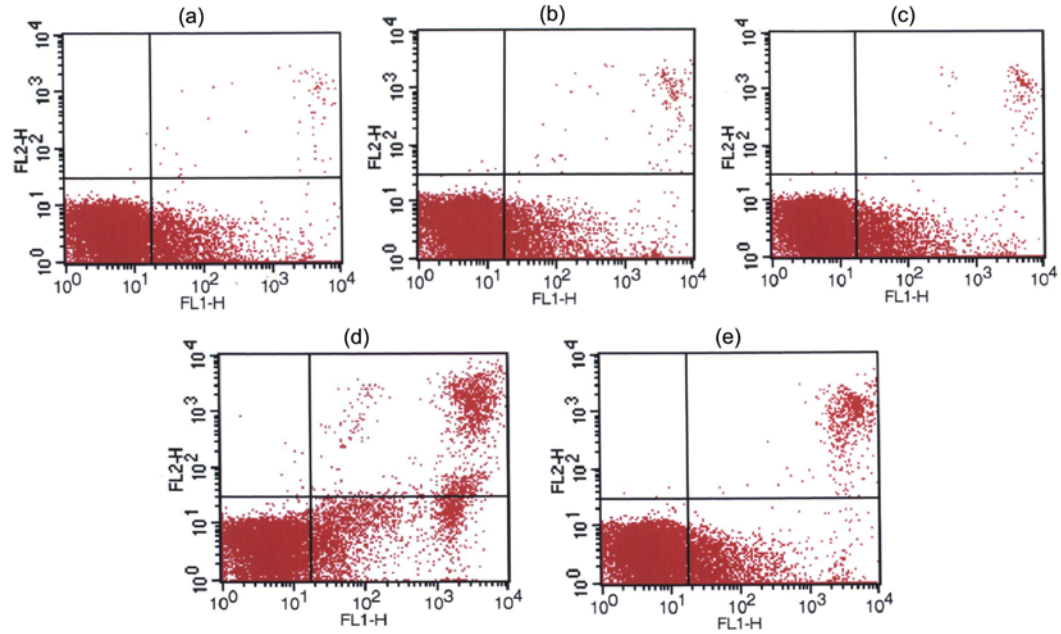

Figure 5. FACS analysis of PBMCs upon treatment with the samples (FL1H: Annexin V FITC and HL2-H: PI): (a) PS, (b) UHMWPE, (c) PC43, (d) ox-UHMWPE, and (e) ox-PC43.

FACS Analysis. In order to examine the population of early and late stage of apoptotic cells, flow cytometry was employed. Figure 5 represents flow cytometry of PBMCs cultured for 48 h on the samples, before and after irradiation, as Annexin V *vs.* PI-A plots with quadrant gates showing four populations. The majority of cells was in the Annexin-PI- (viable and non apoptotic), and the rest were distributed in the Annexin+PI- (early apoptotic) and in the Annexin+PI+ (late apoptotic or necrotic).[19] In the samples before irradiation, no significant difference in cell population was observed compared to (-) control; the populations of cells in early apoptosis were in the range of 26%±2% and in late apoptosis were below 2% (Figure 6(a)). The ox-UHMWPE showed the lowest early apoptosis activity (19%±2%) among the samples, whereas, the ox-PC43 showed almost no difference compared to PC43. It was rather contradictory that ox-UHMWPE, which induced the highest cell death, showed the lowest early apoptosis activity (19%±2%) among the samples. On the other hand, ox-UHMWPE exhibited the highest late apoptosis activity of 11%±2% (Figure 6(b)). Considering this late apoptosis value was 2.75 fold and 5.5 fold higher than ox-PC43-induced and non-irradiated control value, respectively, it was undeniable that the late apoptosis induction was statistically significant. The common feature of such late apoptotic cells is the loss of plasma membrane transport ability to exclude PI.[20] Most apoptotic cells *in vivo* are turned into phagocytes by macrophages or by surrounding cells.[21] However, in the case of PBMCs, further membrane alterations were observed during the late phases of apoptotic cell death, leading to the recognition by additional adaptor molecules.[22] The representatives for those mole-

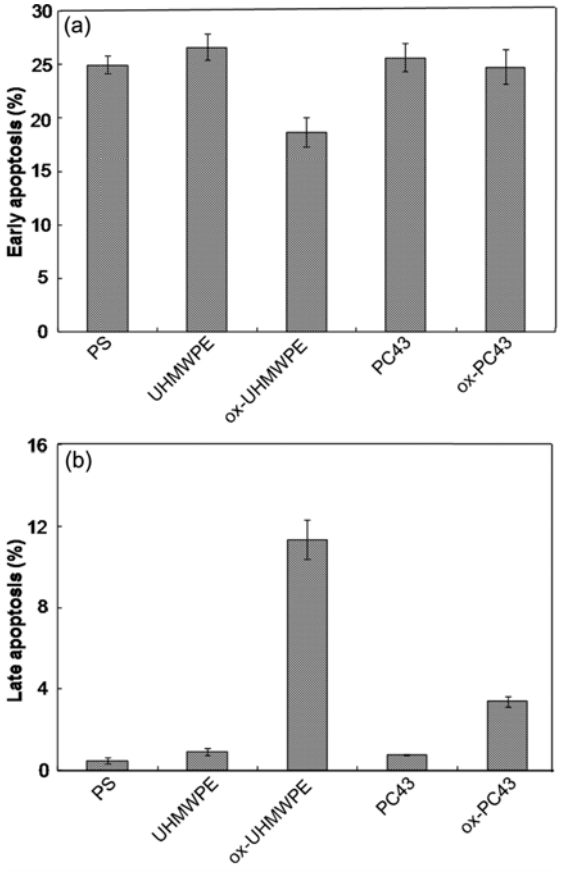

Figure 6. Effects of incubation of the samples on PBMCs percentage: (a) early apoptosis and (b) late apoptosis. The ox-PC43 significantly decreased the late apoptosis percentage of PBMCs compared to ox-UHMWPE.

cules are complement component C1q and C-reactive proteins that activate complement system leading to cell lysis.[23] Consequently, late apoptotic PBMCs *in vivo* can bring about a secondary necrosis characterized by the loss of plasma integrity, in turn, damaging intracellular contents.

Conclusions

ESR studies showed that γ-ray irradiation of the samples generated the free radicals, which were inversely related to zirconia content, and the free radicals strongly influenced the cell viability. DNA fragmentation and DAPI staining assays revealed that the cell death is associated with the induction of apoptosis. Flow cytometry showed that ox-PC43 had a 2.75-fold lower rate of the late apoptosis than ox-UHMWPE. Therefore, it can be concluded that PC43 is the candidate to alleviate secondary necrosis in the prosthetic implants.

Acknowledgment. This work was supported by the Fundamental R&D Program for Technology of World Premier Materials funded by the Ministry of Knowledge Economy, Republic of Korea.

References

(1) L. Costa, M. P. Luda, L. Trossarelli, E. M. Brach del Prever, M. Crova, and P. Gallinaro, *Biomaterials*, **19**, 659 (1998).
(2) L. Fang, Y. Leng, and P. Gao, *Biomaterials*, **26**, 3471 (2005).
(3) M. Goldman, M. Lee, R. Gronsky, and L. Pruitt, *J. Biomed. Mater. Res.*, **37**, 43 (1997).
(4) C. S. Lee, J. Y. Jho, K. Choi, and T. W. Hwang, *Macromol. Res.*, **12**, 141 (2004).
(5) C. S. Lee, S. H. Yoo, J. Y. Jho, K. Choi, and T. W. Hwang, *Macromol. Res.*, **12**, 112 (2004).
(6) F. Medel, E. Gómez-Barrena, F. García-Alvarez, R. Ríos, L. Gracia-Villa, and J. A. Puértolas, *Biomaterials*, **25**, 9 (2004).
(7) F. Reno, F. Lombardi, and M. Cannas, *Biomaterials*, **24**, 17 (2003).
(8) F. Reno, P. Bracco, F. Lombardi, F. Boccafoschi, L. Costa, and M. Cannas, *Biomaterials*, **25**, 6 (2004).
(9) M. Bosetti, L. Zanardi, P. Bocco, L. Costa, and M. Cannas, *Biomaterials*, **24**, 8 (2003).
(10) V. Rincheval, M. Bergeaud, L. Mathieu, J. leory, A. Guillaume, B. Mignotte, N. Le Floch, and J. L. Vayssiere, *Cell Biol. Toxicol.*, Apr. 11 (2012).
(11) G. Denecker, D. Vercammen, W. Declercq, and P. Vandenabeele, *Cell. Mol. Life Sci.*, **58**, 3 (2001).
(12) A. M. Kaufman, C. L. Alabre, H. E. Rubash, and A. S. Shanbhag, *J. Biomed. Mater. Res. A*, **84**, 2 (2008).
(13) S. Kwak, D. I. Noh, H. J. Chun, Y. Mook, Y. C. Nho, J. W. Jang, and Y. B. Shim, *Macromol. Res.*, **17**, 8 (2009).
(14) W. Klopffer, in *Introduction to Polymer Spectroscopy*, Springer-Verlag, New York, 1984, Part D.
(15) K. Nakamura, S. Ogata, and Y. Ikada, *Biomaterials*, **19**, 24 (1998).
(16) M. Slouf, H. Synkova, J. Baldrian, A. Marek, J. Kovarova, P. Schmidt, H. Dorschner, M. Stephan, and U. Gohs, *J. Biomed. Mater. Res. B: Appl. Biomater.,* **85B**, 240 (2008).
(17) B. Halliwell and J. M. C. Gutteridge, in *Free Radicals in Biology and Medicine*, Oxford Univ. Press, Inc., New York, 1999, pp 251-253.
(18) J. Choi, C. Park, J. O. Choi, H. Rhim, and H. J. Chun, *J. Microbiol. Biotechnol.*, **11**, 3 (2001).
(19) R. Hingorani, J. Deng, J. Elia, C. McIntyre, and D. Mittar, in *Application Note: Detection of Apoptosis Using the BD Annexin V FITC Assay on the BD FACSVerse™ System*, BD Biosciences, San Jose, 2011.
(20) Z. darzynkiewicz, G. Juan, X. Li, W. Gorczyca, T. Murakami, and F. Traganos, *Cytometry*, **27**, 1 (1997).
(21) F. Reno, M. Sabbatini, and M. Cannas, *J. Mater. Sci. Mater. Med.*, **14**, 241 (2003).
(22) S. Franz, B. Frey, A. Sheriff, U. S. Gaipl, A. Beer, R. Voll, J. R. Kalden, and M. Herrmann, *Cytometry A*, **69A**, 230 (2006).
(23) H. S. Jang, K. E. Ryu, W. S. Ahn, H. J . Chun, H. D. Park, K. D. Park, and Y. H. Kim, *Colloids Surf. B: Biointerfaces*, **50**, 2 (2006).